Safety, Pharmacokinetics, and Dosimetry of a Long-Acting Radiolabeled Somatostatin Analog ^{177}Lu-DOTA-EB-TATE in Patients with Advanced Metastatic Neuroendocrine Tumors

Jingjing Zhang*[1–3], Hao Wang*[1,3], Orit Jacobson[2], Yuejuan Cheng[4], Gang Niu[2], Fang Li[1,3], Chunmei Bai[4], Zhaohui Zhu†[1,3], and Xiaoyuan Chen†[2]

[1]Department of Nuclear Medicine, Peking Union Medical College Hospital (PUMCH), Chinese Academy of Medical Sciences & Peking Union Medical College (CAMS & PUMC), Beijing, China; [2]Laboratory of Molecular Imaging and Nanomedicine, National Institute of Biomedical Imaging and Bioengineering (NIBIB), National Institutes of Health (NIH), Bethesda, Maryland; [3]Beijing Key Laboratory of Molecular Targeted Diagnosis and Therapy in Nuclear Medicine, Beijing, China; and [4]Oncology Department of Peking Union Medical College Hospital, Chinese Academy of Medical Sciences & Peking Union Medical College (CAMS & PUMC), Beijing, China

Radiolabeled somatostatin analog therapy has become an established treatment method for patients with well to moderately differentiated unresectable or metastatic neuroendocrine tumors (NETs). The most frequently used somatostatin analogs in clinical practice are octreotide and octreotate. However, both peptides showed suboptimal retention within tumors. The aim of this first-in-humans study is to explore the safety and dosimetry of a long-acting radiolabeled somatostatin analog, ^{177}Lu-1, 4, 7, 10-tetra-azacyclododecane-1, 4, 7, 10-tetraacetic acid-Evans blue-octreotate (^{177}Lu-DOTA-EB-TATE). **Methods:** Eight patients (6 men and 2 women; age range, 27–61 y) with advanced metastatic NETs were recruited. Five patients received a single dose, 0.35–0.70 GBq (9.5–18.9 mCi), of ^{177}Lu-DOTA-EB-TATE and underwent serial whole-body planar and SPECT/CT scans at 2, 24, 72, 120, and 168 h after injection. The other 3 patients received intravenous injection of 0.28–0.41 GBq (7.5–11.1 mCi) of ^{177}Lu-DOTATATE for the same imaging acquisition procedures at 1, 3, 4, 24, and 72 h after injection. The dosimetry was calculated using the OLINDA/EXM 1.1 software. **Results:** Administration of ^{177}Lu-DOTA-EB-TATE was well tolerated, with no adverse symptoms being noticed or reported in any of the patients. Compared with ^{177}Lu-DOTATATE, ^{177}Lu-DOTA-EB-TATE showed extended circulation in the blood and achieved a 7.9-fold increase of tumor dose delivery. The total-body effective doses were 0.205 ± 0.161 mSv/MBq for ^{177}Lu-DOTA-EB-TATE and 0.174 ± 0.072 mSv/MBq for ^{177}Lu-DOTATATE. Significant dose delivery increases to the kidneys and bone marrow were also observed in patients receiving ^{177}Lu-DOTA-EB-TATE compared with those receiving ^{177}Lu-DOTATATE (3.2 and 18.2-fold, respectively). **Conclusion:** By introducing an albumin-binding moiety, ^{177}Lu-DOTA-EB-TATE showed remarkably higher uptake and retention in NETs as well as significantly increased accumulation in the kidneys and red marrow. It has great potential to be used in peptide receptor radionuclide therapy for NETs with lower dose and less frequency of administration.

Key Words: peptide receptor radionuclide therapy (PRRT); somatostatin receptor (SSTR); neuroendocrine tumor (NET); Evans blue; TATE

J Nucl Med 2018; 59:1699–1705
DOI: 10.2967/jnumed.118.209841

Because of the body-wide distribution of neuroendocrine cells, neuroendocrine tumors (NETs) are a heterogeneous group of neoplasms that can develop anywhere in the body (*1*). Although NETs are generally categorized as low-grade indolent tumors and other epithelial malignancies, they can be aggressive and resistant to therapy (*2*). Most NETs overexpress somatostatin receptors (SSTRs), so somatostatin analogs are recommended for unresectable and metastatic disease (*3*). However, the clinical efficacy is relatively limited (*4,5*).

For decades, diagnostic radioisotope-labeled somatostatin analogs have been intensively investigated for NET imaging (*6*). With therapeutic radioisotopes such as ^{90}Y or ^{177}Lu, peptide receptor radionuclide therapy (PRRT) has become an established treatment for patients with well to moderately differentiated unresectable or metastatic NETs and disease progression after first-line treatment (*7*). Several phase I and II clinical trials showed favorable results in NETs in general and even better results in patients with gastroenteropancreatic NETs and bronchial NETs, where as much as 30% objective response was observed (*8*). In a recently finished phase III clinical trial, a treatment with ^{177}Lu-DOTATATE resulted in markedly longer progression-free survival and a significantly higher response rate than high-dose octreotide long-acting repeatable (LAR) among patients with advanced midgut NETs (*9*). The promising results from this trial led to the approval of Lutathera (^{177}Lu-DOTA-TATE) by both the European Commission and the U.S. Food and Drug Administration for the treatment of gastroenteropancreatic NETs.

For PRRT, kidneys are usually the critical organs in terms of radiation toxicity due to nonspecific or specific accumulation of radiolabeled peptide, and maximum tolerated dose to kidney is in

Received Feb. 15, 2018; revision accepted Mar. 26, 2018.
For correspondence or reprints contact either of the following:
Zhaohui Zhu, Department of Nuclear Medicine, Peking Union Medical College Hospital, Chinese Academy of Medical Sciences, Beijing 100730, China.
E-mail: 13611093752@163.com
Xiaoyuan Chen, Laboratory of Molecular Imaging and Nanomedicine, National Institute of Biomedical Imaging and Bioengineering (NIBIB), National Institutes of Health, 35A Convent Dr., GD937 Bethesda, MD 20892-3759.
Email: shawn.chen@nih.gov
*Contributed equally to this work.
†Contributed equally to this work.
Published online Apr. 13, 2018.

the range of 23–29 Gy (*10–12*). Renal irradiation is mainly caused by reabsorption of radiolabeled peptides in the proximal tubule. SSTR also plays a role in the total renal uptake of radiolabeled somatostatin analogs (*13*), because vasa recta, tubular cells of the cortex, and distal tubule cells express SSTR (*14,15*). The fast clearance of the peptide also affects the accumulation of radioactivity within the tumor, which means radiolabeled DOTATATE needs to be given by adding intravenous infusion dose and treatment cycles.

As the most abundant plasma protein, serum albumin has emerged as a versatile carrier for therapeutic agents (*16,17*). For example, a DOTA–folate conjugate with a low-molecular-weight albumin-binding entity 4-(*p*-iodophenyl)butyric acid has been designed to prolong its circulation in the blood, leading to improved tumor-to-kidney ratios (*18*). The same albumin-binding-entity–conjugated prostate-specific membrane antigen (PSMA) inhibitor also showed an increased circulation half-life and prostate tumor uptake, compared with the unmodified PSMA inhibitors (*19,20*). Recently, an Evans blue–based albumin-binding moiety was developed as a blood-pool imaging and lymphatic mapping agent (*21–25*) and also for modification of peptides, oligonucleotides, and chemotherapeutic drugs (*26–28*). We also developed a long-acting somatostatin analog (EB-TATE), with the aim to improve the pharmacokinetics and increase therapeutic efficacy (*29*). In a SSTR2-positive AR42J xenograft model, ^{90}Y-DOTA-EB-TATE effectively accumulated in the tumor, resulting in complete regression of the tumors and full survival of the tumor-bearing mice with a single low dose of 3.7 MBq of ^{90}Y-DOTA-EB-TATE (*29*).

Inspired by the promising preclinical results, we conducted a first-in-humans, first-in-class study to explore the safety, tolerability, and dosimetry and preliminary effects of administration of the study drug ^{177}Lu-DOTA-EB-TATE in 5 patients with advanced metastatic NETs. For comparison, ^{177}Lu-DOTA-TATE was evaluated in another 3 patients.

MATERIALS AND METHODS

Patient Recruitment

This is a noncontrolled, nonrandomized, nonblinded first-in-humans study, which was approved by the Institutional Review Board of Peking Union Medical College Hospital, Chinese Academy of Medical Sciences and Peking Union Medical College. This study was registered at clinicaltrials.gov (NCT03308682). All procedures were in accordance with the ethical standards of the institutional and national research committees and with the 1964 Helsinki declaration and its later amendments or comparable ethical standards. A total of 8 patients with metastatic SSTR-expressing NETs were enrolled at Peking Union Medical College Hospital, Beijing.

The inclusion criteria were adult patients with histologically confirmed, metastasized NETs; the tumors being unresectable; identified disease progression according to RECIST (version 1.1); confirmed SSTR expression on the target tumors; and at least one lesion with higher uptake than that of normal liver parenchyma on ^{68}Ga-DOTATATE PET. The exclusion criteria were any of the following: serum creatinine level greater than 150 μM; baseline measured glomerular filtration rate of less than 50 mL/min/1.73 m^2 determined by ^{99m}Tc-DTPA renal function examination; hemoglobin level of less than 8.0 g/dL; white-cell count less than 2.0×10^9/L; platelet count of less than 75×10^9/L; total bilirubin level of greater than 3 times the upper limit of the normal range and serum albumin level of less than 3.0 g/dL; cardiac insufficiency including carcinoid heart valve disease, severe allergy, or hypersensitivity to radiographic contrast material; claustrophobia; and pregnancy or breastfeeding.

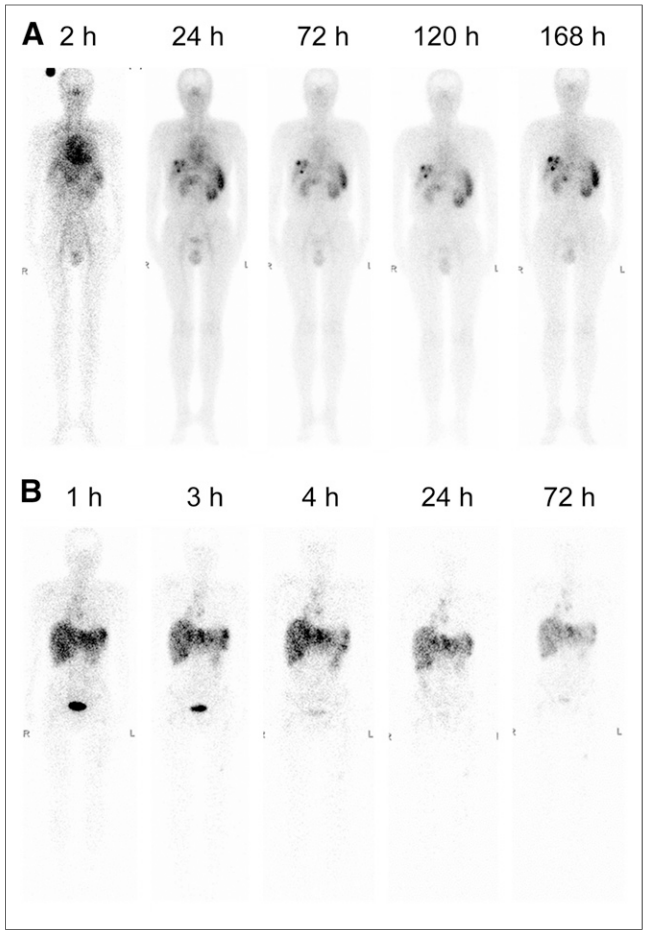

FIGURE 1. (A) Representative whole-body anterior projection images of a 61-y-old male patient with NET liver metastases at 2, 24, 72, 120, and 168 h after intravenous administration of ^{177}Lu-DOTA-EB-TATE. ^{177}Lu-DOTA-EB-TATE cleared from blood pool over time and persistently accumulated in tumors. (B) Representative whole-body anterior projection images of a 49-y-old male patient with NET liver metastases at 1, 3, 4, 24, and 72 h after intravenous administration of ^{177}Lu-DOTA-TATE. ^{177}Lu-DOTATATE showed rapid renal clearance. Tumor uptake also gradually decreased along with time.

PET Procedures

All patients underwent ^{68}Ga-DOTATATE PET/CT scans using a Siemens Biograph 64 True Point system. The emission sequence was initiated at approximately 45 min after intravenous injection of 111–148 MBq (3–4 mCi) of ^{68}Ga-DOTATATE. A Siemens MMWP workstation was used for postprocessing.

Radiopharmaceuticals

DOTA-EB-TATE was synthesized according to the procedure reported previously (*29*). Good-manufacturing-practices–certified, no-carrier-added ^{177}Lu, in the form of $^{177}LuCl_3$, was purchased from LuMark (IDB, Holland). The radiosynthesis was automated on an All-In-One synthesizer. The product (radiochemical purity > 98%) was dissolved in 0.9% saline and passed through a 0.22-μm filter to ensure sterility. The quality control was performed with thin-layer chromatography (BIOSCAN) with CH_3OH:NH_4OAc (v/v 1:1) as the developing solution.

SPECT/CT

No fasting, special diet, hydration, or other specific preparation was requested on the day of ^{177}Lu-DOTA-EB-TATE or ^{177}Lu-DOTATATE injection. Before the injection and 24 h later, safety data were

TABLE 1
Biodistribution of ^{177}Lu-DOTA-EB-TATE (SUV, n = 5) and ^{177}Lu-DOTATATE (SUV, n = 3) in Patients with Advanced NETs

	^{177}Lu-DOTA-EB-TATE				^{177}Lu-DOTA-TATE			
Organ	2 h	24 h	72 h	168 h	1 h	3 h	24 h	72 h
Blood	3.39 ± 1.17	1.75 ± 0.58	1.29 ± 0.44	0.94 ± 0.30	0.17 ± 0.04	0.15 ± 0.02	0.09 ± 0.03	0.03 ± 0.00
Lung	0.41 ± 0.14	0.25 ± 0.09	0.21 ± 0.06	0.14 ± 0.06	0.07 ± 0.02	0.06 ± 0.01	0.05 ± 0.01	0.04 ± 0.01
Liver	1.82 ± 0.73	1.39 ± 0.46	1.27 ± 0.45	1.07 ± 0.41	1.39 ± 0.12	1.25 ± 0.18	0.94 ± 0.09	0.85 ± 0.20
Spleen	3.24 ± 1.50	3.34 ± 1.97	3.54 ± 2.67	3.57 ± 2.97	4.21 ± 0.22	3.93 ± 0.32	3.42 ± 0.52	3.70 ± 0.74
Pancreas	2.23 ± 0.68	1.62 ± 0.45	1.18 ± 0.32	0.98 ± 0.21	0.85 ± 0.23	0.76 ± 0.18	0.57 ± 0.25	0.60 ± 0.22
Kidneys	2.67 ± 0.89	3.03 ± 1.22	3.20 ± 1.86	2.47 ± 1.49	1.78 ± 0.38	1.54 ± 0.22	1.14 ± 0.19	1.13 ± 0.15
Muscle	0.11 ± 0.03	0.17 ± 0.03	0.14 ± 0.04	0.10 ± 0.03	0.09 ± 0.02	0.08 ± 0.03	0.07 ± 0.02	0.07 ± 0.02

Data are mean ± SD.

collected, including physical examination and vital signs, electrocardiography parameters, blood count, biochemistry, and immunology. Any unusual or adverse clinical symptoms were recorded on the day of imaging and during the 3-mo follow-up. Safety data were also measured at 5 d and 1, 2, 4, and 8 wk after the tracer administration. Renal protection was performed using amino acid infusion to hydrate the patients. Before the amino acid infusion, tropisetron hydrochloride was applied to prevent nausea and vomiting. Amino acid infusion (2.5%; 25 g of arginine diluted in 1 L of normal saline) was started 1 h before administration of ^{177}Lu-DOTA-EB-TATE or ^{177}Lu-DOTATATE and maintained over 4 h.

Five patients underwent single-dose administration of ^{177}Lu-DOTA-EB-TATE (0.35–0.70 GBq [9.5–18.9 mCi]), followed by serial whole-body planar and SPECT/CT scans at 2, 24, 72, 120, and 168 h after injection. Another 3 patients accepted intravenous injection of 0.28–0.41 GBq (7.5–11.1 mCi) of ^{177}Lu-DOTA-TATE for the same imaging acquisition procedures at 1, 3, 4, 24, and 72 h after injection. All scans were obtained using a Precedence scanner (Philips Healthcare) with a medium-energy general-purpose collimator and a 20% energy window width centered symmetrically over the 208-keV photopeak of ^{177}Lu.

The whole-body images were acquired with the camera configured for dual-head planar imaging with a 256 × 1,024 matrix at a scan speed of 10 cm/min. SPECT/CT scanning was performed after each whole-body scintigraphy, with each tomographic scan of 32 frames with a 40 sec exposure time per frame (21-min SPECT acquisition time) including all major organs after a low-dose CT scan.

SPECT reconstruction was performed using the system's software on the clinical workstation. An iterative ordered-subset maximum-likelihood expectation maximization algorithm with 3 iterations and 8 subsets was used. Visual analysis was used to determine the general biodistribution and the temporal and intersubject stability. Regions of interest were drawn including the organs and NET lesions on the serial images.

Dosimetry Calculation

The dosimetry calculation was performed according to the European Association of Nuclear Medicine Dosimetry Guidance (*30*) and the procedure reported previously (*23*). A radioactive source with a well-determined ^{177}Lu activity at a fixed position near the top of head on whole-body planar images was used to calculate dose concentration factor, and voxel-based activity concentration was converted to SUV in the volumes of interest. The decay uncorrected time–activity curve was generated based on the SUV of each organ. The SUVs were then converted to MBq/MBq on the basis of organ weight from the adult male phantom and the adult female phantom provided by the OLINDA/EXM (version 1.1; Vanderbilt University, USA) (*31,32*). The time-integrated activity coefficient of each organ was determined by fitting the data using a biphase exponential model provided by the software. The residence times of the urine bladder and NETs were calculated by the trapezoidal method using GraphPad Prism (version 4.0; GraphPad Software, Inc.). The void time was set as 60 min. The volume of left ventricle was set as 550 mL to calculate the residence of heart content. The ratio of activity mass concentrations for red marrow to blood was set as 0.32 to calculate dose delivery to bone marrow (*33*). The effective doses were calculated by entering the time-integrated activity coefficient for all source organs into OLINDA/EXM for either a 73.7 kg adult male or a 56.9 kg adult female. All the data were expressed as mean ± SD.

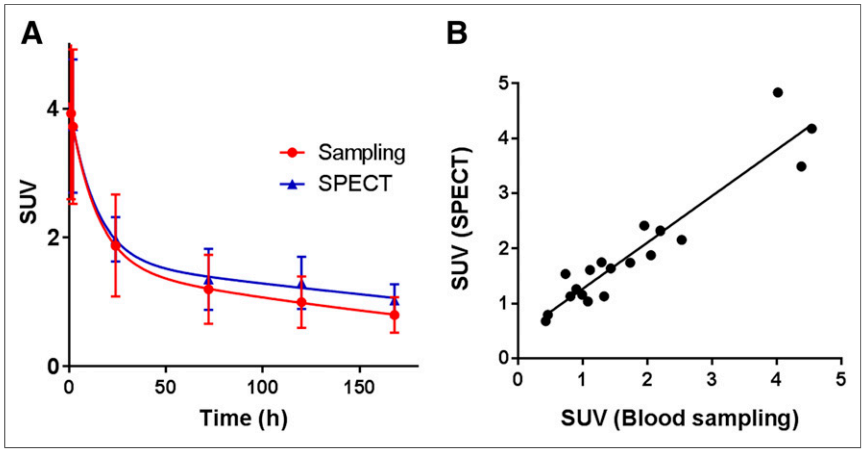

FIGURE 2. (A) Blood clearance of ^{177}Lu-DOTA-EB-TATE quantified by SPECT and γ-counting of blood samples. (B) There is positive linear correlation between SPECT quantification and blood sampling (R^2 = 0.90, P < 0.0001).

RESULTS

Safety Profile

All patient information is included in Supplemental Table 1 (supplemental materials are available at http://jnm.snmjournals.org). With a mean injected dose of 0.632 ± 0.079

GBq (17.08 ± 2.14 mCi) of ^{177}Lu-DOTA-EB-TATE or 0.28–0.41 GBq (7.5–11.1 mCi) of ^{177}Lu-DOTA-TATE, no subjective side effects were experienced, and no adverse symptoms were noticed or reported. No clinically significant changes on physical examination, electrocardiography parameters, blood count, biochemistry, and immunology during the entire 7-d procedure and 3-mo follow-up in any of the patients were found.

Pharmacokinetics Profile

At 2 h after injection, ^{177}Lu-DOTA-EB-TATE showed a relatively high level in the blood, as indicated by the strong signal in the heart region and major vessels (Fig. 1A). Among normal organs, liver, spleen, and kidneys showed moderate uptake of ^{177}Lu-DOTA-EB-TATE. ^{177}Lu-DOTATATE also showed moderate uptake in the liver, spleen, and kidneys, but no apparent uptake in the blood circulation was detected (Fig. 1B). Both agents showed negative brain uptake. On the basis of the quantitative data summarized in Table 1, ^{177}Lu-DOTA-EB-TATE showed a much higher retention in the blood (SUV, 1.75 ± 0.58) than ^{177}Lu-DOTATATE (SUV, 0.09 ± 0.03) at 24 h after injection ($P < 0.01$). The uptake of ^{177}Lu-DOTA-EB-TATE in the lung, liver, kidneys, and muscle was also higher than those of ^{177}Lu-DOTA-TATE. The uptake in the spleen was similar for the 2 agents.

To confirm the accuracy of SPECT quantification, blood samples were collected from the patients at different time points after TATE injection, and radioactivity within the blood samples was quantified using a γ-counter. A positive and significant correlation between SPECT quantification and blood sampling was observed ($R^2 = 0.90$, $P < 0.0001$, Fig. 2).

Normal Organ Dosimetry

On the basis of the quantification of SPECT images, dosimetry was calculated using OLINDA/EXM software (Table 2). As to the whole-body effective dose, there was no significant difference between ^{177}Lu-DOTA-EB-TATE and ^{177}Lu-DOTATATE (0.080 ± 0.05 vs. 0.069 ± 0.032 mSv/MBq, $P > 0.05$). The spleen was the organ that received the highest absorbed dose for both agents, with 1.45 ± 1.59 mSv/MBq for ^{177}Lu-DOTA-EB-TATE and 1.77 ± 0.95 mSv/MBq for ^{177}Lu-DOTATATE, respectively. ^{177}Lu-DOTA-EB-TATE had a significantly higher effective dose in the kidneys than ^{177}Lu-DOTATATE (1.15 ± 0.92 vs. 0.36 ± 0.07 mSv/MBq,

TABLE 2
Estimated Effective Dose After Intravenous Administration of ^{177}Lu-NOTA-EB-TATE ($n = 5$, 4 Men and 1 Woman) and ^{177}Lu-DOTATATE ($n = 3$, 2 Men and 1 Woman)

Target organ	^{177}Lu-DOTA-EB-TATE (mSv/MBq)	^{177}Lu-DOTATATE (mSv/MBq)
Adrenals	0.0099 ± 0.0062	0.0063 ± 0.0023
Brain	0.0004 ± 0.0001	0.0002 ± 0.0001
Breasts	0.0016 ± 0.0006	0.0010 ± 0.0004
Gallbladder wall	0.0106 ± 0.0046	0.0068 ± 0.0024
Lower large intestine wall	0.0032 ± 0.0013	0.0020 ± 0.0007
Small intestine	0.1596 ± 0.0698	0.0712 ± 0.0171
Stomach wall	0.0896 ± 0.0317	0.0501 ± 0.0121
Upper large intestine wall	0.0062 ± 0.0029	0.0035 ± 0.0010
Heart wall	0.1918 ± 0.0512	0.0475 ± 0.0308
Kidneys	1.1494 ± 0.9183	0.3603 ± 0.0677
Liver	0.3468 ± 0.1531	0.2247 ± 0.0954
Lungs	0.0479 ± 0.0178	0.0095 ± 0.0033
Muscle	0.0375 ± 0.0159	0.0260 ± 0.0137
Ovaries	0.0040 ± 0.0016	0.0023 ± 0.0008
Pancreas	0.2872 ± 0.1044	0.4143 ± 0.1153
Red marrow	0.0582 ± 0.0137	0.0032 ± 0.0004
Osteogenic cells	0.0329 ± 0.0118	0.0033 ± 0.0009
Skin	0.0013 ± 0.0005	0.0009 ± 0.0003
Spleen	1.4470 ± 1.5894	1.7693 ± 0.9450
Testes	0.0011 ± 0.0003	0.0010 ± 0.0005
Thymus	0.0026 ± 0.0008	0.0015 ± 0.0006
Thyroid	0.0015 ± 0.0004	0.0010 ± 0.0005
Urinary bladder wall	0.0204 ± 0.0141	0.0635 ± 0.0388
Total body	0.0370 ± 0.0176	0.0243 ± 0.0089
Effective dose equivalent	0.2048 ± 0.1605	0.1735 ± 0.0722
Effective dose	0.0804 ± 0.0500	0.0693 ± 0.0317

Data are mean ± SD.

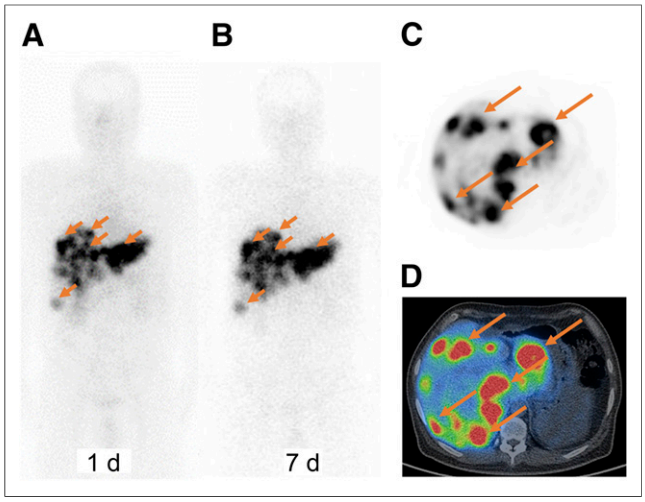

FIGURE 3. ^{68}Ga-DOTATATE PET/CT and ^{177}Lu-DOTA-EB-TATE whole-body planar imaging and SPECT/CT of a 45-y-old male NET patient with multiple liver metastases. (A) Liver metastases identified by ^{68}Ga-DOTATATE PET were clearly visualized on whole-body anteroposterior projection image at 1 d after administration of ^{177}Lu-DOTA-EB-TATE. (B) Liver metastases were still clearly visualized on whole-body anteroposterior projection image at 7 d after administration of ^{177}Lu-DOTA-EB-TATE. (C and D) Multiple liver metastases were shown on axial PET image (C) and PET/CT (D) at 45 min after intravenous injection of ^{68}Ga-DOTATATE.

$P < 0.01$). ^{177}Lu-DOTA-EB-TATE also showed higher exposure to red bone marrow than ^{177}Lu-DOTATATE (0.058 ± 0.014 vs. 0.0032 ± 0.0004 mSv/MBq, $P < 0.01$). ^{177}Lu-DOTATATE showed higher exposure to pancreas and urinary bladder wall than ^{177}Lu-DOTA-EB-TATE.

Dose Delivery of ^{177}Lu-DOTA-EB-TATE to NET Lesions

As shown in Figures 3 and 4, NET lesions were clearly identified with ^{68}Ga-DOTATATE, with high local accumulation of radioactive signals at 45 min after injection. Most of the lesions seen by ^{68}Ga-DOTATATE PET were also visualized on ^{177}Lu-DOTA-EB-TATE and ^{177}Lu-DOTATATE planar images and SPECT. It is worth noting that even at day 7, the NET lesions still showed high retention of radioactivity on ^{177}Lu-DOTA-EB-TATE SPECT whereas the tumor uptake of ^{177}Lu-DOTATATE decreased remarkably at 24 h after injection.

In 5 patients with NET, a total 25 lesions were identified on ^{177}Lu-DOTA-EB-TATE SPECT, including 1 primary lesion in the pancreas, 18 liver metastases, 5 lymph node metastases, and 1 pancreas metastasis. The average SUVs of these lesions were 9.91 ± 6.15, 14.91 ± 8.66, 22.28 ± 13.40, 22.46 ± 12.95, and 21.94 ± 11.63 at 2, 24, 72, 120, and 168 h after injection, respectively. In 3 patients with NET, a total of 37 lesions were identified on ^{177}Lu-DOTATATE SPECT, including 1 lung metastasis, 21 liver metastases, 9 lymph node metastases, 4 bone metastases, and 2 pelvic metastases. The average SUVs of these lesions were 7.58 ± 5.07, 8.37 ± 5.63, 7.67 ± 5.34, 5.25 ± 3.19, and 3.86 ± 2.10 at 1, 3, 4, 24, and 72 h after injection, respectively. In patients receiving ^{177}Lu-DOTA-EB-TATE, the average tumor SUV of ^{68}Ga-DOTATATE PET was 12.37 ± 4.92, which was significantly lower than that in patients receiving ^{177}Lu-DOTATATE (17.49 ± 7.02, $P < 0.05$).

Tumor uptake of ^{177}Lu-DOTATATE reached the peak at a very early time (3 h after injection) and decreased over time, whereas that of ^{177}Lu-DOTA-EB-TATE kept increasing from 2 to 120 h and remained high between 120 and 168 h (Fig. 5A). Consequently, in patients receiving ^{177}Lu-DOTA-EB-TATE, the number of disintegration of the ^{177}Lu in the tumor region by mass average was 0.0469 ± 0.0167 MBq-h/MBq/g, which was about 7.9-fold higher than that in patients receiving ^{177}Lu-DOTATATE (0.0059 ± 0.0033 MBq-h/MB/g, $P < 0.01$) (Fig. 5B). In both ^{177}Lu-DOTA-EB-TATE and ^{177}Lu-DOTATATE scans, the number of disintegration in NETs correlated well with the SUV determined by ^{68}Ga-DOTATATE PET.

DISCUSSION

In this first-in-humans study, a recently developed long-lasting SSTR targeting agent (*29*), ^{177}Lu-DOTA-EB-TATE, was applied in patients with advanced NETs. No subjective side effects were experienced, and no adverse symptoms were noticed or reported, indicating the safety of ^{177}Lu-DOTA-EB-TATE.

Because of albumin binding, ^{177}Lu-DOTA-EB-TATE showed a relatively long circulation half-life, with $t_{1/2}\alpha$ around 9.47 h and $t_{1/2}\beta$ around 236 h ($t_{1/2}\alpha$ = plasma/distribution half life; $t_{1/2}\beta$ = tissue/elimination

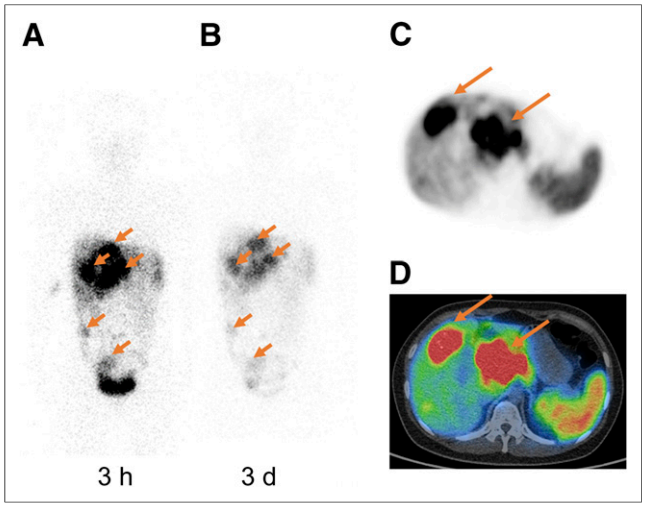

FIGURE 4. ^{68}Ga-DOTATATE PET/CT and ^{177}Lu-DOTATATE whole-body planar imaging and SPECT/CT in a 27-y-old woman with advanced NET (G2). Multiple liver metastases were shown on whole-body anteroposterior projection images at 3 h (A) and 3 d (B) after administration of ^{177}Lu-DOTATATE. Same liver metastases were shown on axial PET (C) and PET/CT (D) at 45 min after intravenous injection of ^{68}Ga-DOTATATE.

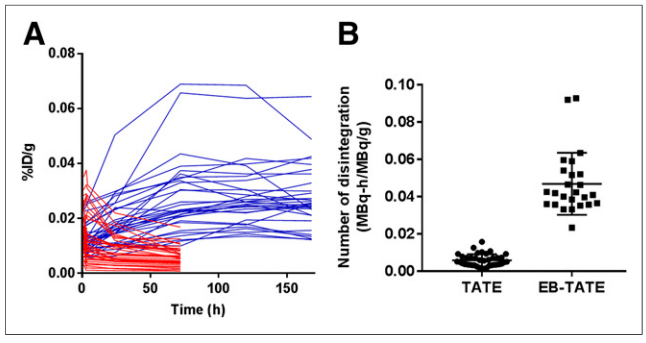

FIGURE 5. (A) Time–activity curves of NET lesions after administration of ^{177}Lu-DOTA-EB-TATE (blue) and ^{177}Lu-DOTATATE (red). (B) Number of disintegration of ^{177}Lu within NET lesions from ^{177}Lu-DOTA-EB-TATE and ^{177}Lu-DOTATATE.

half-life). Prolonged blood retention of ^{177}Lu-DOTA-EB-TATE led to increased whole-body distribution over ^{177}Lu-DOTATATE. Consequently, radiation exposure to red marrow from ^{177}Lu-DOTA-EB-TATE reached 0.058 ± 0.014 mSv/MBq, which is 18.2-fold that of ^{177}Lu-DOTATATE. It is well accepted that PRRT induces hematologic toxicity, usually resulting from bone marrow exposure to radioactivity. Indeed, subacute grade 3–4 hematologic toxicity was observed in 11% of the patients after PRRT with ^{177}Lu-DOTATATE (*34*). A recent study revealed that the prevalence of persistent hematologic dysfunction after PRRT was 4% in 274 GEP NET patients receiving ^{177}Lu-DOTATATE (*35*). On the basis of a generally accepted maximum absorbed dose of 2 Gy to the bone marrow (*36*), up to 33 GBq of ^{177}Lu-DOTA-EB-TATE can be given to a patient. However, in view of the poor correlation between mean absorbed dose to the bone marrow and developed hematologic toxicity (*8*), the real therapy protocol has to be carefully planned. Plus, radiation exposure of the spleen may also affect the development of hematologic toxicity (*37*). Both ^{177}Lu-DOTA-EB-TATE and ^{177}Lu-DOTATATE showed high spleen accumulation, which may be explained by SSTR2 expression in this organ (*13*).

For PRRT, the maximum tolerated dose to kidneys is in the range of 23–29 Gy (*10–12*). Renal irradiation is mainly caused by reabsorption of radiolabeled peptides in the proximal tubule. SSTR also plays a role in the total renal uptake of radiolabeled somatostatin analogs (*13*), because endogenous expression of SSTR2s was found in vasa recta, tubular cells of the cortex, and distal tubule cells (*14,15*). Different from ^{177}Lu-DOTA-TATE, which showed high dose rate within the early time period, ^{177}Lu-DOTA-EB-TATE showed rather steady and extended kidney accumulation over time. Consequently, the absorbed dose in the kidneys for ^{177}Lu-DOTA-EB-TATE was higher than that of ^{177}Lu-DOTATATE. The retention of ^{177}Lu- DOTA-EB-TATE in the kidneys is likely attributed to prolonged circulation, renal clearance, reabsorption in the proximal tubule, and SSTR2 expression. Because DOTA-EB-TATE has a much longer circulating time than DOTATATE, 2.5% L-arginine infusion may not show enough kidney protection. Other strategies may be needed to further reduce kidney retention of radiometal labeled DOTA-EB-TATE.

One limitation of this study is that the number of patients is rather small. A therapy study with more patients is necessary to compare ^{177}Lu-DOTA-EB-TATE with ^{177}Lu-DOTATATE with regard to therapeutic efficacy and potential toxicity. Moreover, all the recruited patients had been heavily treated, receiving various therapy regimens before undergoing DOTA-EB-TATE SPECT/CT. The dose calculation of normal organs may be affected by the high uptake in the tumors.

CONCLUSION

By introducing an albumin-binding moiety, ^{177}Lu-DOTA-EB-TATE showed significantly higher NET uptake and retention over ^{177}Lu-DOTATATE. This first-in-humans study demonstrates that ^{177}Lu-DOTA-EB-TATE is safe and well tolerated in NET patients.

DISCLOSURE

This work was supported in part by the Intramural Research Program (IRP) of the National Institute of Biomedical Imaging and Bioengineering (NIBIB), National Institutes of Health (NIH), the Key Project on Inter Governmental International Scientific and Technological Innovation Cooperation in National Key Projects of Research and Development Plan (2016YFE0115400), National Natural Science Foundation of China projects (81701742, 81741142), and Beijing Municipal Natural Science Foundation (7161012). No other potential conflict of interest relevant to this article was reported.

ACKNOWLEDGMENTS

We thank Prof. Hongyan Ying (Oncology Department, PUMCH, CAMS & PUMC) for helpful regulatory advices, Dr. Yeqing Liu and Dr. Hongtao He (Philips Healthcare) for help in SPECT quantification, Dr. Hui Li (Department of Nuclear Medicine, PUMCH, CAMS & PUMC) for image acquisition, Dr. Xiaoping Hu (Beijing PET Technology Co., Ltd) and Dr. Dayong Huang (Tiansi Information Technology Co., Ltd.) for radiolabeling, and Dr. Jiahua Xu (GE Healthcare) for SPECT data analysis.

REFERENCES

1. Modlin IM, Oberg K, Chung DC, et al. Gastroenteropancreatic neuroendocrine tumours. *Lancet Oncol.* 2008;9:61–72.
2. Nikou GC, Angelopoulos TP. Current concepts on gastric carcinoid tumors. *Gastroenterol Res Pract.* 2012;2012:287825.
3. Wolin EM. The expanding role of somatostatin analogs in the management of neuroendocrine tumors. *Gastrointest Cancer Res.* 2012;5:161–168.
4. Keskin O, Yalcin S. A review of the use of somatostatin analogs in oncology. *Onco Targets Ther.* 2013;6:471–483.
5. Tartarone A, Lerose R, Aieta M. Somatostatin analog therapy in small cell lung cancer. *Semin Nucl Med.* 2016;46:239–242.
6. Barrio M, Czernin J, Fanti S, et al. The impact of somatostatin receptor-directed PET/CT on the management of patients with neuroendocrine tumor: a systematic review and meta-analysis. *J Nucl Med.* 2017;58:756–761.
7. Kwekkeboom DJ, Krenning EP. Peptide receptor radionuclide therapy in the treatment of neuroendocrine tumors. *Hematol Oncol Clin North Am.* 2016;30:179–191.
8. Bodei L, Cremonesi M, Kidd M, et al. Peptide receptor radionuclide therapy for advanced neuroendocrine tumors. *Thorac Surg Clin.* 2014;24:333–349.
9. Strosberg J, El-Haddad G, Wolin E, et al. Phase 3 trial of ^{177}Lu-Dotatate for midgut neuroendocrine tumors. *N Engl J Med.* 2017;376:125–135.
10. Del Prete M, Buteau FA, Beauregard JM. Personalized ^{177}Lu-octreotate peptide receptor radionuclide therapy of neuroendocrine tumours: a simulation study. *Eur J Nucl Med Mol Imaging.* 2017;44:1490–1500.
11. Kwekkeboom DJ, de Herder WW, Kam BL, et al. Treatment with the radiolabeled somatostatin analog [^{177}Lu-DOTA^{0},Tyr^{3}]octreotate: toxicity, efficacy, and survival. *J Clin Oncol.* 2008;26:2124–2130.
12. Cives M, Strosberg J. Radionuclide therapy for neuroendocrine tumors. *Curr Oncol Rep.* 2017;19:9.
13. Rolleman EJ, Kooij PP, de Herder WW, Valkema R, Krenning EP, de Jong M. Somatostatin receptor subtype 2-mediated uptake of radiolabelled somatostatin analogues in the human kidney. *Eur J Nucl Med Mol Imaging.* 2007;34:1854–1860.
14. Reubi JC, Horisberger U, Studer UE, Waser B, Laissue JA. Human kidney as target for somatostatin: high affinity receptors in tubules and vasa recta. *J Clin Endocrinol Metab.* 1993;77:1323–1328.
15. Balster DA, O'Dorisio MS, Summers MA, Turman MA. Segmental expression of somatostatin receptor subtypes sst_1 and sst_2 in tubules and glomeruli of human kidney. *Am J Physiol Renal Physiol.* 2001;280:F457–F465.
16. Elsadek B, Kratz F. Impact of albumin on drug delivery–new applications on the horizon. *J Control Release.* 2012;157:4–28.
17. Liu Z, Chen X. Simple bioconjugate chemistry serves great clinical advances: albumin as a versatile platform for diagnosis and precision therapy. *Chem Soc Rev.* 2016;45:1432–1456.
18. Müller C, Struthers H, Winiger C, Zhernosekov K, Schibli R. DOTA conjugate with an albumin-binding entity enables the first folic acid-targeted ^{177}Lu-radionuclide tumor therapy in mice. *J Nucl Med.* 2013;54:124–131.
19. Choy CJ, Ling X, Geruntho JJ, et al. ^{177}Lu-labeled phosphoramidate-based PSMA inhibitors: the effect of an albumin binder on biodistribution and therapeutic efficacy in prostate tumor-bearing mice. *Theranostics.* 2017;7:1928–1939.
20. Benešová M, Umbricht CA, Schibli R, Muller C. Albumin-binding PSMA ligands: optimization of the tissue distribution profile. *Mol Pharm.* 2018;15:934–946.
21. Niu G, Lang L, Kiesewetter DO, et al. *In vivo* labeling of serum albumin for PET. *J Nucl Med.* 2014;55:1150–1156.

22. Wang Y, Lang L, Huang P, et al. *In vivo* albumin labeling and lymphatic imaging. *Proc Natl Acad Sci USA.* 2015;112:208–213.
23. Zhang J, Lang L, Zhu Z, Li F, Niu G, Chen X. Clinical translation of an albumin-binding PET radiotracer ^{68}Ga-NEB. *J Nucl Med.* 2015;56:1609–1614.
24. Long X, Zhang J, Zhang D, et al. Microsurgery guided by sequential preoperative lymphography using ^{68}Ga-NEB PET and MRI in patients with lower-limb lymphedema. *Eur J Nucl Med Mol Imaging.* 2017;44:1501–1510.
25. Chen H, Tong X, Lang L, et al. Quantification of tumor vascular permeability and blood volume by positron emission tomography. *Theranostics.* 2017; 7:2363–2376.
26. Zhu G, Lynn GM, Jacobson O, et al. Albumin/vaccine nanocomplexes that assemble in vivo for combination cancer immunotherapy. *Nat Commun.* 2017;8:1954.
27. Chen H, Jacobson O, Niu G, et al. Novel "add-On" molecule based on Evans blue confers superior pharmacokinetics and transforms drugs to theranostic agents. *J Nucl Med.* 2017;58:590–597.
28. Zhang F, Zhu G, Jacobson O, et al. Transformative nanomedicine of an amphiphilic camptothecin prodrug for long circulation and high tumor uptake in cancer therapy. *ACS Nano.* 2017;11:8838–8848.
29. Tian R, Jacobson O, Niu G, et al. Evans blue attachment enhances somatostatin receptor subtype-2 imaging and radiotherapy. *Theranostics.* 2018;8:735–745.
30. Lassmann M, Chiesa C, Flux G, Bardies M. EANM Dosimetry Committee guidance document: good practice of clinical dosimetry reporting. *Eur J Nucl Med Mol Imaging.* 2011;38:192–200.
31. Roivainen A, Kähkönen E, Luoto P, et al. Plasma pharmacokinetics, whole-body distribution, metabolism, and radiation dosimetry of ^{68}Ga bombesin antagonist BAY 86-7548 in healthy men. *J Nucl Med.* 2013;54:867–872.
32. Wang Z, Zhang M, Wang L, et al. Prospective study of ^{68}Ga-NOTA-NFB: radiation dosimetry in healthy volunteers and first application in glioma patients. *Theranostics.* 2015;5:882–889.
33. Wessels BW, Bolch WE, Bouchet LG, et al. Bone marrow dosimetry using blood-based models for radiolabeled antibody therapy: a multiinstitutional comparison. *J Nucl Med.* 2004;45:1725–1733.
34. Bergsma H, Konijnenberg MW, Kam BL, et al. Subacute haematotoxicity after PRRT with ^{177}Lu-DOTA-octreotate: prognostic factors, incidence and course. *Eur J Nucl Med Mol Imaging.* 2016;43:453–463.
35. Bergsma H, van Lom K, Raaijmakers M, et al. Persistent hematologic dysfunction after peptide receptor radionuclide therapy with ^{177}Lu-DOTATATE: incidence, course, and predicting factors in patients with gastroenteropancreatic neuroendocrine tumors. *J Nucl Med.* 2018;59:452–458.
36. Forrer F, Krenning EP, Kooij PP, et al. Bone marrow dosimetry in peptide receptor radionuclide therapy with [^{177}Lu-DOTA^{0},Tyr^{3}]octreotate. *Eur J Nucl Med Mol Imaging.* 2009;36:1138–1146.
37. Svensson J, Hagmarker L, Magnander T, Wangberg B, Bernhardt P. Radiation exposure of the spleen during ^{177}Lu-DOTATATE treatment and its correlation with haematological toxicity and spleen volume. *EJNMMI Phys.* 2016;3:15.

The Journal of NUCLEAR MEDICINE

Safety, Pharmacokinetics, and Dosimetry of a Long-Acting Radiolabeled Somatostatin Analog ^{177}Lu-DOTA-EB-TATE in Patients with Advanced Metastatic Neuroendocrine Tumors

Jingjing Zhang, Hao Wang, Orit Jacobson, Yuejuan Cheng, Gang Niu, Fang Li, Chunmei Bai, Zhaohui Zhu and Xiaoyuan Chen

J Nucl Med. 2018;59:1699-1705.
Published online: April 13, 2018.
Doi: 10.2967/jnumed.118.209841

The Journal of Nuclear Medicine is published monthly.
SNMMI | Society of Nuclear Medicine and Molecular Imaging
1850 Samuel Morse Drive, Reston, VA 20190.
(Print ISSN: 0161-5505, Online ISSN: 2159-662X)

SNMMI SOCIETY OF NUCLEAR MEDICINE AND MOLECULAR IMAGING